# A Predictive Model for the $[Rh_2(esp)_2]$ -catalyzed Intermolecular C(sp³)-H Bond Insertion of $\beta$ -carbonyl Ester Carbenes: Interplay Between Theory and Experiment

Brett D. McLarney, a Steven R. Hanna, Djamaladdin G. Musaev, b, and Stefan France, a Company of the Brett D. McLarney, a Steven R. Hanna, Djamaladdin G. Musaev, b, and Stefan France, a Company of the Brett D. McLarney, a Company of the Brett D. M

**ABSTRACT:** Intermolecular  $C(sp^3)$ -H insertions of β-carbonyl ester dirhodium carbenes are extremely rare. Toward developing efficient reactions of these carbenes, a model for their insertion into  $C(sp^3)$ -H bonds is described using DFT calculations. In this study, the relevant electronic and steric components of β-carbonyl ester dirhodium carbenes that affect intermolecular  $C(sp^3)$ -H activation energies are explored, parameterized, and used to construct an intuitive model for predicting propensity for C-H insertion. The resulting insights from the theoretical investigation are actualized through with experiments to establish reactivity trends for these species and reaction discovery. Based on these integrated computational and experimental efforts, examples of intermolecular  $C(sp^3)$ -H insertion featuring secondary α-diazo-β-amide esters are reported. The resulting carbenes feature an intramolecular 1,6-hydrogen bond that affords increased stability and enhanced reactivity for  $C(sp^3)$ -H insertion as compared to other β-carbonyl ester dirhodium carbenes. The reactivity of these carbenes is also highlighted through (1) an example of a cyclopropanation reaction, and (2) the use of a chiral dirhodium catalyst system.

**Keywords:** C-H Functionalization, Predictive Model, Dirhodium Acceptor-Acceptor carbenes, Density Functional Theory, Parametrization of Stereoelectronic Effects

# 1. Introduction

Diazo-derived metal-carbenes have been a cornucopia of synthetically useful reactivity. The reactivity of these species prominently features C-H and X-H bond activation, cyclopropanation, and a host of [3+2] cycloaddition chemistry.<sup>1-9</sup> Metal-carbene compounds have been subdivided between five categories: acceptor only (A), acceptor-acceptor (A-A), donor-acceptor (D-A), donor-donor (D-D), and donor only (D) (Figure 1). To date, studies on D-A carbenoids feature a panoply of selective C(sp3)-H functionalization chemistry in which the donor group is credited with stabilizing the metal-carbene interaction.10 On the other hand, whilst their functional diversity renders them a promising source of synthetic building blocks, A-A diazo compounds have found little application in the budding field of intermolecular selective C(sp³)–H functionalization chemistry due to several challenges.

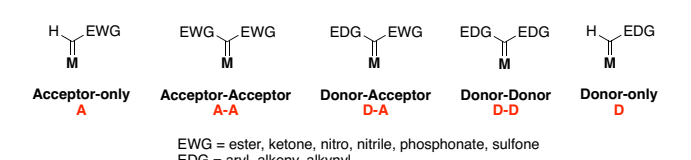


Figure 1. Classifications of metal-carbene compounds

These challenges include but are not limited to: (a) high energy barriers for A-A diazo decomposition, or nitrogen extrusion (requiring more active catalysts); (b) weak metal-carbene interactions (resulting in low enantioselectivities due to catalyst dissociation);10,11 and (c) relatively small singlet-triplet energy splitting in the A-A carbenes (providing undesired conformational changes and differential reactivities). 12,13 These challenges often preclude the A-A carbenes from regio- and stereoselective addition to nucleophiles. Moreover, they make the A-A carbenoids prone to side reactions (e.g., Wolff rearrangements, 4 ylide formation and rearrangement, 5 beta-lactam formation, 6 H-atom abstraction, <sup>17</sup> etc.) which create complex mixtures in reaction vessels. For this reason, the vast majority of C-H functionalization reactions that feature A-A diazo compounds are performed intramolecularly.5,18 Previous studies on their intramolecular C(sp³)-H functionalization and

<sup>&</sup>lt;sup>a</sup> School of Chemistry and Biochemistry, Georgia Institute of Technology, Atlanta, Georgia 30332

<sup>&</sup>lt;sup>b</sup> Cherry L. Emerson Center for Scientific Computation and Department of Chemistry, Emory University, 1515 Dickey Drive, Atlanta, Georgia 30322

<sup>&</sup>lt;sup>c</sup> Petit Institute of Bioengineering and Bioscience, Georgia Institute of Technology, Atlanta, Georgia 30332

cyclopropanation revealed that chemo- and regioselectivity of A-A carbene reactivity is highly sensitive to the identity of the acceptor groups. <sup>5,16,19,20,21</sup> However, understanding the roles of the steric bulkiness and electronic nature of functional groups in the previously studied intramolecular reactions failed to offer generalizable rules/concepts for intermolecular C(sp³)–H functionalization.

Therefore, this paper investigates the reactivity of dirhodium(tetracarboxylate)-carbene complexes (derived from A-A diazo compounds) with alkane substrates in an aim to develop generalized predictive rules for their effective utilization in selective intermolecular  $C(sp^3)$ –H functionalization reactions. Previous investigations of intermolecular  $C(sp^3)$ –H functionalization reactions have focused solely on carbenes derived from dimethyl diazomalonate<sup>6</sup> and thus similarly lack comprehensiveness. <sup>22,23</sup> As such, little is known on the influence of the nature of the acceptor groups on A-A carbene  $C(sp^3)$ –H insertion in an intermolecular dirhodium(tetracarboxylate)-catalyzed manifold.

Given the challenges regarding utilization of A-A dirhodium-carbenes in intermolecular C(sp³)-H functionalization, we turned to density functional theory (DFT) studies to systematically probe acceptor group modifications in an aim to guide our complex experiments. To simplify the discussion and provide a reasonable starting point (with directly comparable parameters), the  $\beta$ -carbonyl ester class of A-A dirhodium carbenes will serve as the focus of this study. In a seminal study, Nakamura et al. modeled the dirhodium(tetraformate)-catalyzed C(sp³)-H functionalization between alkanes and methyl diazoacetate or diazomethane (Figure 2A).24 This work demonstrated that, in a C-H insertion transition state mediated by dirhodium-carbenes, positive charge accumulates on the C-H bond donor while negative charge accumulates on the carbene unit. In this sense, C-H insertions are heuristically viewed as concerted hydride transfer and carbocation trapping process. This view has been supported by experimental evidence showing that reactions are faster for benzylic and alphaheteroatom C-H bond donors than for those containing only aliphatic C-H bonds.<sup>25</sup>

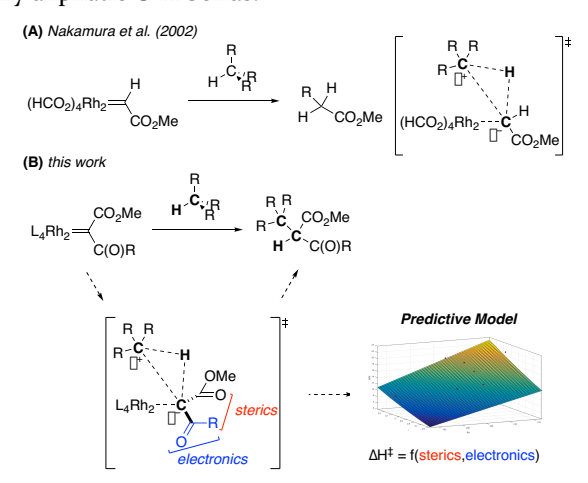


**Figure 2**. Dirhodium-carbene insertion into  $C(sp^3)$ -H bond as described by Nakamura (**A**) and this work (**B**).

In the spirit of the findings by Nakamura and co-workers, herein, we hypothesized that the difference in C-H activation energies for various dirhodium-carbenes of β-carbonyl esters could be explained by two factors. First, the ability of the carbonyl groups to stabilize negative charge accumulation at the carbene carbon center that is anticipated to have a stabilizing effect on the C(sp³)–H insertion transition state, consequently, lowering the activation energy. Second, allylic strain between the carbonyl substituent and ester in the C-H insertion transition state is, in contrast, expected to have a destabilizing effect. Encouraged by previously reported predictive reactivity models,<sup>26</sup> in this paper, using DFT, we the divide barrier of the dirhodium β-carbonyl ester carbene insertion into C(sp³)-H bonds into two orthogonal steric and electronic components (Figure 2B). These components of the C-H insertion barrier are directly related to the specific nature of the carbonyl substituent. Therefore, the reactivity of the dirhodium β-carbonyl ester carbene was quantified by changing the carbonyl substituent and examining effects on the stereoelectronic components. This acquired knowledge was then used to build a map of chemical space, as a predictive model, highlighting subcategories of the β-carbonyl ester class of A-A carbenes in terms of their propensity for C(sp<sup>3</sup>)-H insertion. Ultimately, this predictive model is validated through experimental evidence and led to discovery of the dirhodium secondary N-aryl  $\alpha$ -diazo- $\beta$ -amide esters carbene that is highly reactive toward C(sp³)-H bonds.

# 2. Computational Methods

Geometry optimizations and frequency calculations for all reported structures were performed at the Mo6L level of density functional theory in conjunction with 6-31G(d,p) basis sets for H, C, N, O, F and Cl atoms and LANL2DZ basis set and corresponding Hay-Wadt effective core potential for Rh.<sup>27</sup> Each reported minimum has confirmed to have zero imaginary frequencies and each transition state (TS) structure to have only one imaginary frequency associated with the reaction coordinate. Intrinsic reaction coordinate (IRC) calculations were performed for selected transition state structures to confirm their true identity. Bulk solvent effects are incorporated using the self-consistent reaction field polarizable continuum model (IEF-PCM) with dichloromethane as the solvent.<sup>28</sup> The calculated Gibbs free energies are corrected to a solution standard state of 1M at room temperature (298.15K). To minimize redundant discussion, below we discuss only the calculated enthalpies. Enthalpy values are generally more reliable than Gibbs free energies (which depends on concentration related parameters and more) and thus considered to be advantageous for establishing meaningful trends. Electronic energies (with and without zero-point-corrections) and Gibbs free energies are provided in the Supporting Information.

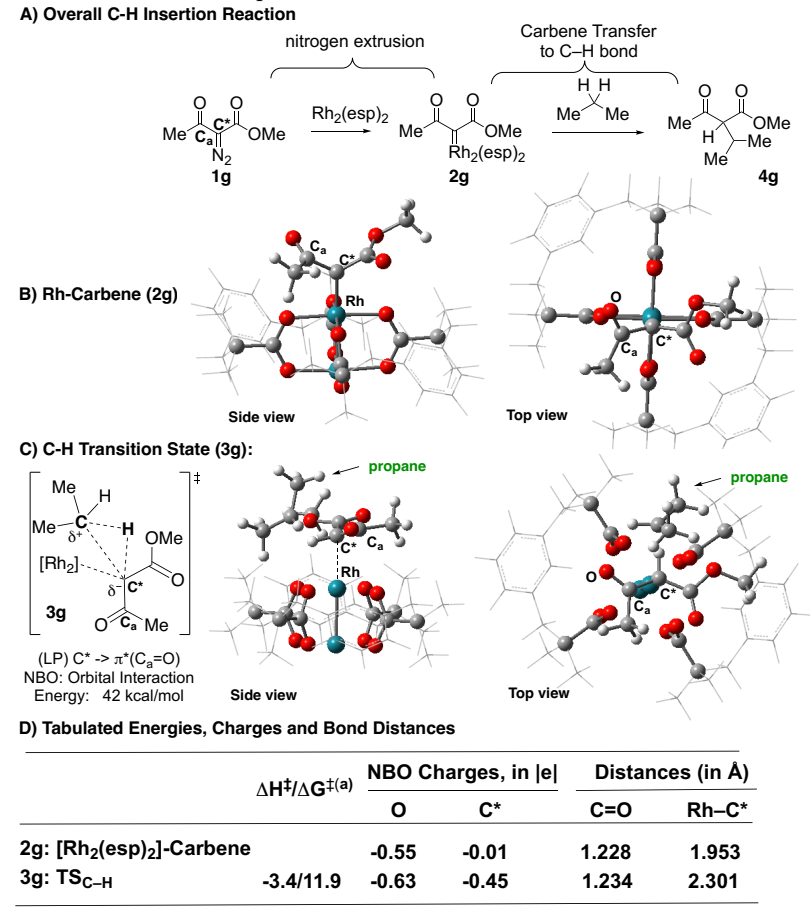
## 3. An Instructive Model Study

To elucidate the governing factors of A-A carbene transfer from the metal-carbene complex to the C–H bond of the substrate, we studied the (a)  $[Rh_2(esp)_2]$ -carbene complex (2g) derived from the reaction of  $\alpha$ -diazo methyl

acetoacetate (1g) and Rh<sub>2</sub>(esp)<sub>2</sub>, and the (b) transition state (3g) associated with the carbene transfer from 2g to the C–H bond of propane (Figure 3). DFT calculations demonstrated that in carbene transfer transition state 3g, positive charge accumulates on the carbon of the activated C-H bond while negative charge accumulates on the C\* center of carbene unit: the calculated NBO charges of the C\* center are -0.01 |e| and -0.45 |e| for 2g and 3g, respectively (Figure 3C). Notably, we found that the lone-pair (LP) of the carbene carbon strongly interacts with the  $\pi^*$  orbital of the adjacent carbonyl, C<sub>a</sub>=O, in the insertion transition state, which impacts the charge distribution at the C\* center. In 3g, compared to 2g, the ester carbonyl assumed an anti-periplanar ("down") conformation with respect to the

incoming propane; meanwhile, the ketone carbonyl preferred a *syn*-periplanar ("up") conformation. This orientation presumably allows for optimal dipole alignment as well as to eschew steric interactions between the ketone substituent and the propane due to increasing 1,2-allylic strain in the transition state.

Intrigued by these analyses and results, we set forth an in-depth investigation into the impact, both electronic and steric, of the ketone substituent (R) on the charge distribution at the C\*-center, as well as disruption of the preferred anti-periplanar orientation of the  $\beta$ -carbonyl ester carbenoid. Below, we developed the tools to decouple electronic and steric effects, and study their impact independently.



(a) Calculated Relative to [Rh2(esp)2]-carbene + Substrate, and given in kcal/mol

**Figure 3.** (**A**) Overall C-H insertion reaction studied in this paper, (**B**)  $[Rh_2(esp)_2]$ -carbene complex derived from the reaction of α-diazo methyl acetoacetate and  $[Rh_2(esp)_2]$ -catalyst, (**C**) the C-H insertion transition state **3g**, and (**D**) Calculated NBO charges of carbonyl oxygen and carbene carbon, selective bond distances, and relative energy (in kcal/mol) of the transition state **3g**.

# 3.1 Quantifying Electronic Effects

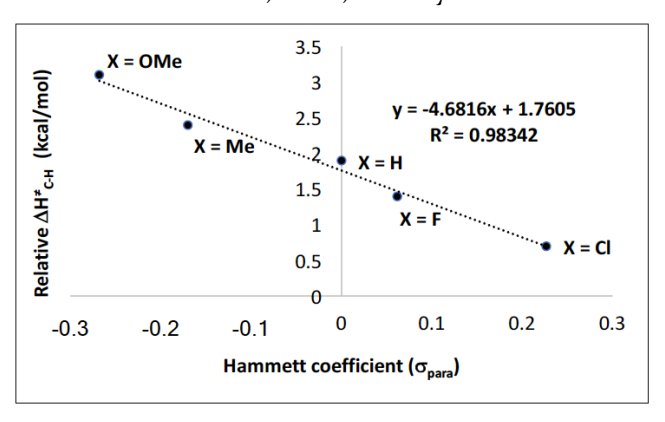
To quantify electronic effects, we studied the  $[Rh_2(esp)_2]$ -carbene complexes (**2a-e**) of a series  $\beta$ -ketoesters with p-substituted phenyl ketone groups. By choosing p-substituted phenyl ketones, we essentially minimize any steric effects and isolate the electronic ones. The transition states (**3a-e**) associated with metal-carbene transfer to the

C–H bond of propane were modeled and calculated (relative to the reactants,  $[Rh_2(esp)_2]$ -carbene + propane, Figure 4). At first, we used the well-established Hammett coefficient,  $\sigma_p$ , to assess the effect of negative charge accumulation at the carbene carbon on the energy of the transition state.<sup>29</sup>

**Figure 4**. Hammett coefficients and C-H insertion energies for aryl  $\beta$ -ketoester carbenes **2a-e** 

We found a direct correlation ( $R^2=0.98342$ ) between Hammett coefficient and the activation barriers at the carbene transfer transition states **3a-e** (Figure 5). For instance, with an activation enthalpy of  $\Delta H^{\ddagger}=3.1$  kcal/mol, the p-methoxyphenyl ketone **2a** has the smallest  $\sigma_p$ . In contrast, the p-chlorophenyl ketone **2e** with  $\Delta H^{\ddagger}=0.5$  kcal/mol has the largest  $\sigma_p$ . In general, as the phenyl ring becomes electron deficient, the C-H activation barrier decreases and Hammett coefficient increases. These findings allow us to conclude that the electronic nature of the carbonyl [i.e.  $\pi^*(C_\alpha=O)$ –LP( $C^*$ ) interaction] plays an important role in determining the C-H activation barriers at the carbene transfer transition state.

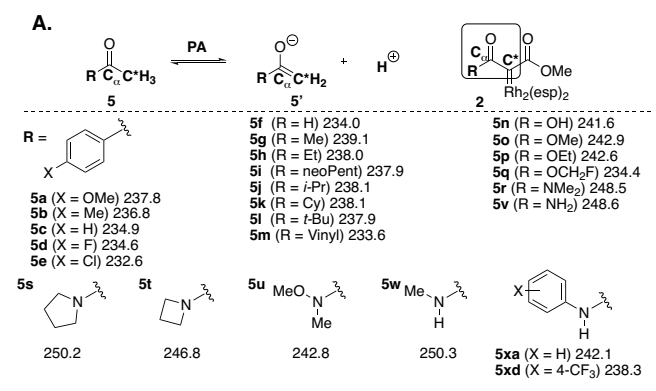
Since the Hammett coefficients only apply to substituted phenyl rings, other parameters had to be considered to quantify the general ability of a carbonyl substituent to stabilize negative charge accumulation on the carbene. A representative example is shown by comparing the dirhodium carbenes of the 4-chlorophenyl-containing β-ketoester **2e** and methyl acetoacetonate 2g, the initial model system. Given that phenyl ketones are generally considered to be more electron poor than methyl ketones, one would expect the 4-chlorophenyl system 2e to have a lower C-H activation barrier. However, calculations showed that its activation barrier ( $\Delta H^{\ddagger}$  = 0.5 kcal/mol) is higher than that of the methyl acetoacetate **2g** ( $\Delta H^{\ddagger} = -3.4 \text{ kcal/mol}$ ). Therefore, we continued to search for a universal parameter that would better represent electronic effects across phenyl ketones as well as amides, esters, and alkyl ketones.



**Figure 5.** Relative activation enthalpy (in kcal/mol) vs Hammett coefficient.

Next, proton affinity (PA) was explored as a potential electronic parameter (Figure 6).<sup>30</sup> We calculated PAs for a

variety of methyl-substituted carbonyls **5** (as a mimic of the C\* carbon center of the metal-carbene complex **2**) and compared the values to the C-H insertion favorability of the corresponding full transition states **3** (Figure 6B). Lower PAs correspond to electron-poor carbonyls while higher PAs suggest electron-rich carbonyls. Along these lines, the acetophenones (**5a-5e**) and acetaldehyde (**5f**) were among the most electronically deficient carbonyl acceptor groups (with PAs = 232.6–237.8 kcal/mol) while amides (**5r-5x**) were among the most electron-rich (with PAs = 238.3-250.2 kcal/mol). Most of the simple alkyl ketones (**5g-5l**) had PA ranges between 237.9 and 239.1 kcal/mol, whereas higher PAs were observed for esters (**50-5q**).



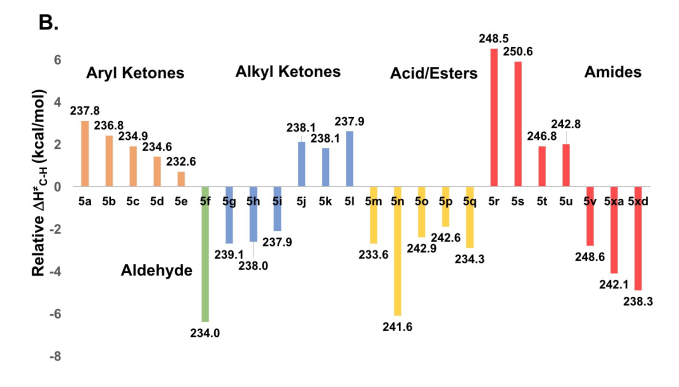


**Figure 6**. **(A)** Calculated proton affinities (PAs, in kcal/mol) of the substrates examined and **(B)** a schematic presentation of relative activation enthalpy (in kcal/mol) and proton affinity for each substrate and class.

Employing Nakamura's hydridic C–H insertion mechanistic framework, one should expect that more electron-poor carbenes (with lower PAs) will react faster than the electron-rich ones (with higher PAs). Representatives of each carbonyl type were selected to establish a hierarchy of electronic properties of the  $\beta$ -carbonylester carbenes and their reactivity with C-H bonds as a function of the nature of the carbonyl substituent (Figure 7). For the selected molecules, the following trend was observed: aldehyde (5f) < phenyl ketone (5c) < methyl ketone (5g) < methyl ester (5o) < dimethyl amide (5r). This order matches well with well-established carbonyl electrophilicity rules and directly associates with the C–H activation energy. Thus, if we were to assume that the sterics of the system had no impact on the C-H alkylation transition state, then alde-

hydes would be expected to have the lowest C(sp³)-H alkylation barriers and amides the highest. However, it should be noted that the PA values within each carbonyl classes have broader ranges, can be impacted by other groups of the metal-carbene complex, and may overlap. For example, replacing a hydrogen with a fluorine on the methyl ester (i.e. 5q, the CH₃-to-CH₂F substitution) reduces PA of carbene carbon by 8 kcal/mol and makes it more reactive toward C–H bond. Therefore, PA should be used with caution because it does not solely explain energy trends within a carbonyl class or across all calculated substrates.

Increasing PA; Decreasing electrophilicity; Decreasing favorability for C-H functionalization

**Figure 7**. Representative substrates and their calculated PA parameters (in kcal/mol).

# 3.2 Quantifying Steric Effects

In the literature, steric effects of organic molecules are typically parameterized by A-values, which are derived from the 1,3-diaxial interactions on cyclohexane rings.<sup>31</sup> Hypothesizing that the 1,5 R•••O steric interaction in the [Rh<sub>2</sub>(esp)<sub>2</sub>]-carbenoid is analogous to the 1,3-diaxial strain on cyclohexane rings, we examined the relationship between available literature A-values of alkyl groups and the calculated C–H activation energies of the carbene transfer transition state 3 (Figure 8).

$$\begin{bmatrix} [Rh_2] & \delta^y \\ 0 & 0 \\ R & 0 \end{bmatrix} \longrightarrow \begin{bmatrix} R & H \\ R & A-value \end{bmatrix}$$

**Figure 8**. Schematic presentation of the used A-value parameter.

To assess impact of steric effects while eschewing complexity from electronic effects, a sterically diverse set of alkyl ketone carbenes with a narrow PA range (237.9 – 239.1 kcal/mol) was selected (Figure 9). To directly compare the steric effects in the alkyl ketones systems with that of an aryl ketone system, we chose the 4-methoxyphenyl ketone carbene 2a as the representative aryl substrate given its similar electronic nature (PA = 237.8 kcal/mol) to the selected alkyl ketone carbenes. Since literature A-values for the 4-substituted phenyl substituents are not available, in our analyses, we used the A-value of 3.00, which corresponds to the phenyl (i.e., unsubstituted) group.

**Figure 9.** A-Values and relative activation enthalpies of the C–H insertion transition states **3** for some members of the alkyl series

A correlation ( $R^2 = 0.6893$ ) exists between A-value and the calculated C-H activation energies for the selected series of R groups – the larger A-value (i.e. larger steric effect) the higher energy of the transition state (Figure 9). However, there are some inconsistencies that warrant further discussion. In the isopropyl (3i) and cyclohexyl (3k) cases, dramatically different activation barriers are found despite both having the same A value of 2.15. The isopropyl group can rotate to relieve steric interactions with the dirhodium catalyst. In contrast, the size and rigidity of the cyclohexyl chair conformation results in destabilizing steric interactions with the dirhodium catalyst that are not reflected in the A-value determination. Another example of the inconsistencies is shown by the *t*-butyl group (31 with A = 4.5). Despite having a higher A-value than the 4-OMe-phenyl group 3a, 3l has a slightly lower  $\Delta H$  value ( $\Delta \Delta H = 0.5$ kcal/mol). In this case, the relative destabilization of the C-H activation TS for 31 caused by the 1,5 R ••• O repulsion is compensated by stabilizing interactions between the *t*-butyl group and dirhodium catalyst in the [Rh2(esp)2]-carbene complex.

Thus, while A-value represents a good parameter to estimate steric effects in some cases, it has limitations and is not available for many R groups. To circumvent this issue, we introduced a new and more general geometric parameter,  $\mathbf{r}$ , defined as the distance between the carbonyl substituent, R, and the ester carbonyl oxygen in the C–H insertion transition state (Figure 10A). As seen in Figure 10B, this parameter correlates well ( $R^2 = 0.98$ ) with the A-values of the R groups discussed above (see Supporting Information Figure S6).

# A. Defining the parameter r [Rh2] + OME R O 3 B. Relationship between A-value and r

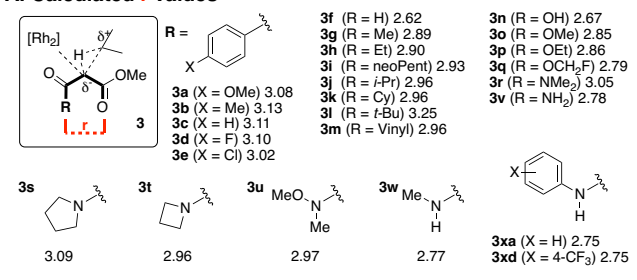
[Rh<sub>2</sub>] 
$$\stackrel{\delta \gamma}{\longrightarrow}$$
 OMe R O 3  $\stackrel{\dagger}{\longrightarrow}$  R<sup>2</sup> = 0.98 R H A-value extendable accessible

**Figure 10.** Defining the parameter  $\mathbf{r}(\mathbf{A})$  and its relationship to A-value (**B**).

These findings encouraged us to use **r** as a general parameter for assessing the impact of steric effect on the transition state of the metal-carbene insertion into the C–H bond. Using the same substrates examined for PA calculations (see above), **r** values were determined and grouped

by type of carbonyl substituent (Figure 11). A steric hierarchy was then constructed to represent the severity of the 1,5 steric interactions in the C-H insertion transition state. Thus, more severe 1,5-strain would result in a larger  $\bf r$ , and less strain would result in a smaller  $\bf r$ . As a representative example, for the aliphatic ketones (3 $\bf g$ -3 $\bf l$ ), we found that the t-butyl ketone (3 $\bf l$ ) had the most 1,5-strain in the C-H insertion transition state and the largest  $\bf r$  (3.25 Å), while the methyl ketone (3 $\bf g$ ), with the smallest  $\bf r$ , had the least 1,5-strain. Comparatively, as expected, the aldehyde (3 $\bf f$ ) had even lower steric strain with  $\bf r$  = 2.62 Å.

#### A. Calculated r values



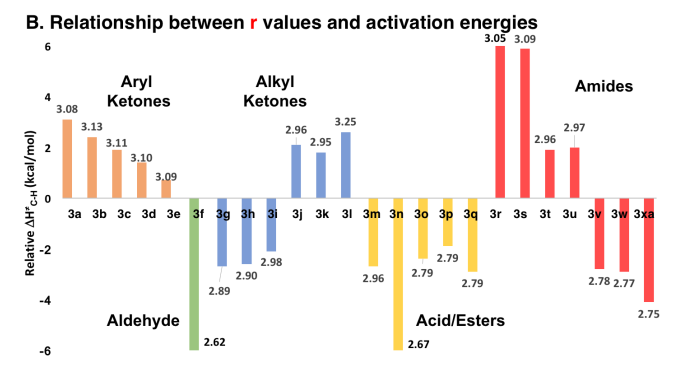


**Figure 11**. Calculated **r** values (in Å) for substrates examined (**A**) and to relation to relative activation energies (**B**).

Overall, the calculations have established that the phenyl ketones (3a-3e) had more steric strain when compared to the aliphatic ketones as their r values ranged between 3.02-3.13 Å. With the ability to rotate steric bulk away from the ester in the transition state, the aliphatic ketones (3g-3l) are expected to lower strain than the phenyl groups, which prefer coplanarity with the carbonyl. The esters (3o-3q) followed with r values between 2.79 and 2.85 Å. Steric bulk on the esters is distally located and thus has little contribution to steric strain in the transition state. *tert*-Amides (3r-3u) overlapped with this range with the dimethyl amide (3r) having a larger r value of 3.05 Å. Tethering the amide alkyl groups reduces the steric strain as evinced by the

azetidine group (**3t**, **r** = 2.96 Å), which had strain equal to the isopropyl ketone (**3j**). Interestingly, the secondary amides (**3v-3x**) have **r** values (2.75-2.78 Å) that are 0.2-0.3 smaller than the *tert*-amides, but on par with the alkyl ketones. For instance, upon replacing one N-methyl group in dimethyl amide **3r** with a hydrogen (as in **3w**), a 0.3 Å decrease in **r** value is seen. Close analyses suggest the presence of a 1,6-hydrogen bonding interaction (discussed in detail in Section 5).

## 4. A Predictive Model

# 4.1. Mapping Chemical Space

Having introduced parameters allowing deconstruction of the steric and electronic effects impacting the  $[Rh_2(esp)_2]$ -catalyzed  $\beta$ -carbonyl ester carbene insertion into the  $C(sp^3)$ -H bond, we next aimed to develop a general predictive model. This model is expected to predict carbonyl substituents that will facilitate the C–H insertion. For this purpose, we represent relative enthalpy,  $\Delta H$ , of the C-H insertion transition state 3 as a function of PA and  $\bf r$  parameters,  $\Delta H = f(PA, {\bf r})$ , and interpolate this function using a two-dimensional spline.<sup>32</sup> (see Supporting materials, Figure S11).

The 2D representation of the resulting chemical-space map with different  $\beta$ -carbonyl ester substrates (R) is given in Figure 12. As seen from this Figure, the aryl ketones (**3a-e**) are located on the upper left part of the map and have  $\Delta H$  values > 0. The alkyl/vinyl ketones (**3f-m**) are spread across the left half of the map and have varied negative  $\Delta H$  values which depend on  $\bf r$ . Carboxylic acid  $\bf 3n$  and esters (**30-q**) are located on the lower half of the map with  $\Delta H <$  0. For the most part, the amides (**3r-x**) are clustered on the right half of the map and display varied  $\Delta H$  values. Interestingly, the amides split into separate regions based on substitution, with the tertiary amides (**3r-u**) in the upper right and the secondary ones (**3v-x**) mainly in the bottom right.

From these observations, the existence of four major classes of carbenes becomes apparent. Each class is grouped together into specific locations on the surface, which allows the map to be divided into four sections or quadrants.

*Quadrant 1* (**Q1**) contains the most electronically rich (PA>242) and sterically hindered carbenes, with  $\Delta H^{\ddagger}_{\text{C-H}}$  > 0. The tertiary amides are the representative compound class in **Q1**.

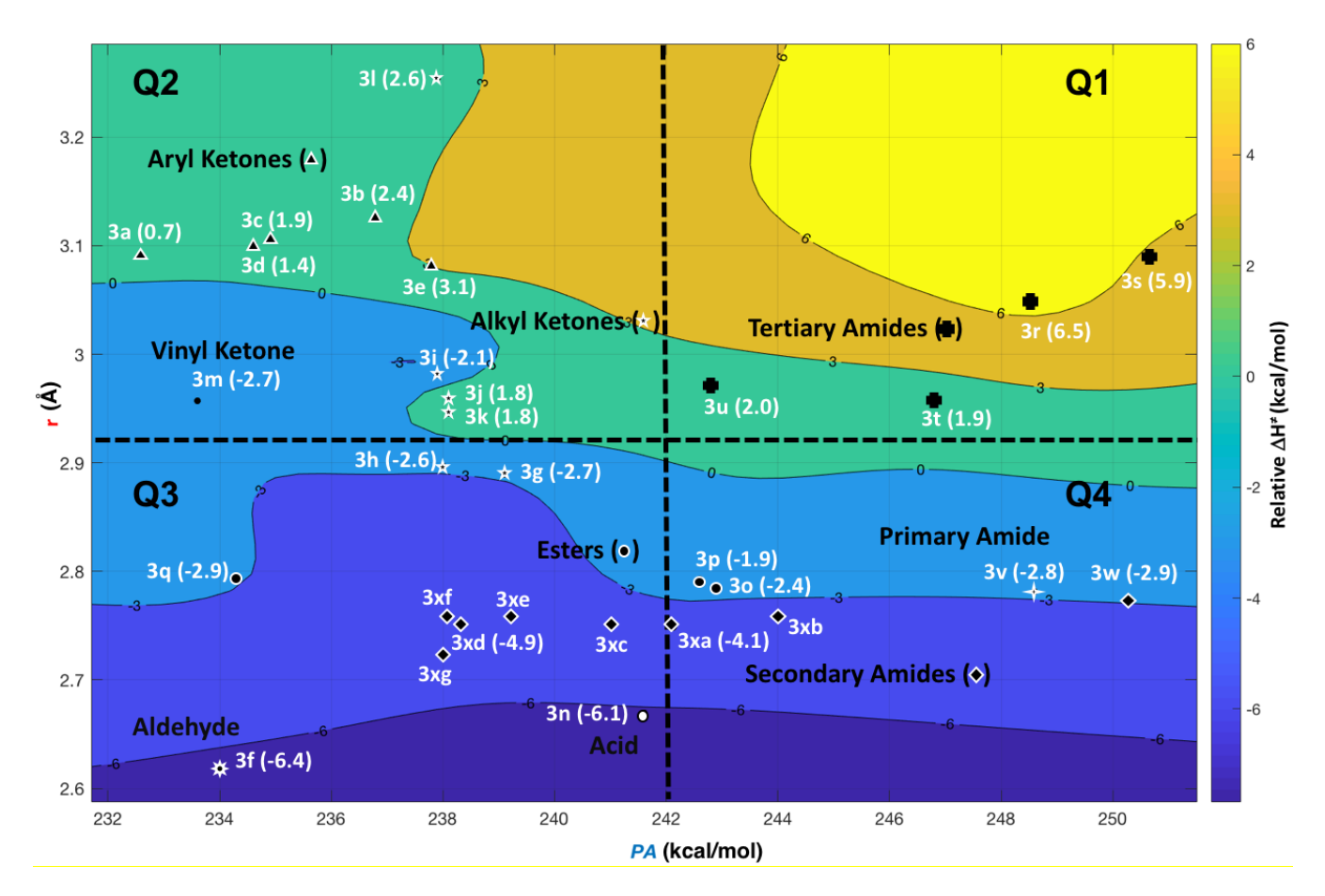


**Figure 12.** Contour map showing calculated relationships between steric ( $\mathbf{r}$ ) and electronic ( $\mathbf{PA}$ ) parameters, and enthalpy ( $\Delta H$ , in kcal/mol) of the C-H insertion transition states 3.

*Quadrant* 2 (**Q2**) contains sterically hindered but electron poor (PA<242) carbenes such as phenyl ketones (**3a-e**) and alkyl ketones (**3i-l**) where the alkyl group is particularly bulky (e.g., R = neopentyl, *i*-Pr, Cy, *t*-Bu). Carbenes in **Q2** have  $\Delta H^{\ddagger}_{C-H} > -1$  kcal/mol.

Quadrant 3 (Q3) contains electron poor and sterically unhindered carbenes such as the aldehyde 3f, simple alkyl ketones (3g/h, R= Me, Et), carboxylic acid 3n, esters bearing electron-withdrawing substituents (i.e., 3q, where R = OCH<sub>2</sub>F), and secondary amides with electron-withdrawing N-aryl groups (3xc-3xg). Due to either reduced steric bulk or that bulk being rotated away from the carbonyl oxygen in the transition state, the aldehyde, simple alkyl ketones, and esters have smaller r values. In contrast, the carboxylic acid and the secondary amides have smaller r values due to the presence of 1,6-hydrogen bonding. This, ultimately, leads to relative activation enthalpies that are negative ( $\Delta H^{\dagger}_{C-H}$  <0).

Quadrant 4 (Q4) houses electron-rich and sterically unhindered carbenes such as esters 30/p, the primary amide 3v, and secondary amides with electron-rich *N*-aryl groups (e.g., 3xa and 3xb). Q4 also has negative activation enthalpies. While each of these species has a smaller r value for one of the reasons discussed above, all have higher PAs due to lone pair donation into the carbonyl.

Interpretation: The developed map of chemical space approach (i.e. predictivity model) is envisioned to aid chemists in building β-carbonyl ester dirhodium carbenoids with better C-H insertion reactivity. Steric factors seem to more directly correlate with relative enthalpies, while electronic factors can be used to tune and modulate reactivity. The steric component determines whether a species is Q1/Q2 or Q3/Q4 (top or bottom half of map). Conversely, the electronic component determines whether a species is Q2/Q3 or Q1/Q4 (left or right half of map). Further strength of the map lies in the ability to properly capture stereoelectronic trends within substrate classes. For example, the parent N-phenyl secondary amide species 3xa corresponds to a Q4 system. By incorporating an electron withdrawing group on the *N*-aryl group (as in **3xd**, where aryl = 4-CF<sub>3</sub>-Ph), the change in PA properly reflects the change to a more electron-poor system, resulting in a shift from Q4 to Q3. A similar shift is observed with esters 30/p vs 3q. Thus, by performing calculations of PA and r for a proposed carbene then identifying where it would fall on the map (Q1-Q4), chemists can gauge the carbene's feasibility for C-H insertion and use it to guide further carbene design.

# 4.2. Making the Model Accessible

For this map to have utility beyond rationalizing observable trends (i.e. to be predictive), calculating both PA and **r** value must be straightforward and not time-consuming.

While PA can be easily and accurately calculated, access to r values requires time-intensive and complicated calculations of the large dirhodium carbene complexes and related C-H insertion transition states. Thus, unless a chemist has access to high-level computing capabilities, this model would not be useful. To address this limitation while making the proposed model more accessible, we developed another steric parameter, r' (Figure 13). r' represents the R-O distance in the anion of the corresponding β-carbonyl ester (6). r' can be easily calculated using commercial molecular modeling softwares (e.g., Spartan, Macromodel, etc.). Taking the t-butyl ketone as a representative example, a close similarity is observed between A-value, r, and r', with r and r' differing by ~0.04 Å (see Supporting materials). Furthermore, we have shown that r and r' parameters are closely correlated ( $R^2 = 0.96$ ) for the above presented carbenes (see Supporting materials). It is important to note that while  $\mathbf{r}'$  is a close approximation of  $\mathbf{r}$ , it does not account for any added interactions and influences due to the dirhodium catalyst and/or the substrate in transition state 3. Given this fact, throughout the remainder of our studies, we continue to use r as the appropriate steric parameter.

OME R<sup>2</sup> = 0.96 
$$\begin{bmatrix} [Rh_2] & 8 \\ 0 & 3 \end{bmatrix}$$
  $\stackrel{\mathbb{R}^2 = 0.98}{\Longrightarrow}$   $\stackrel{\mathbb{R} \setminus \{H\}}{\Longrightarrow}$   $\stackrel{\mathbb{R}^2 = 0.98}{\Longrightarrow}$   $\stackrel{\mathbb{R} \setminus \{H\}}{\Longrightarrow}$   $\stackrel{\mathbb{R}^2 = 0.98}{\Longrightarrow}$  extendable, easily computed

**Figure 13.** Relationship between A-value, and r and r' parameters

# 5. Experimental Validation of the Proposed Model

To test the predictive power of the proposed reactivity model, we first studied the reaction of aryl  $\alpha$ -diazo- $\beta$ -ketoesters with Rh<sub>2</sub>(esp)<sub>2</sub> in neat, refluxing cyclohexane (Scheme 1). Each reaction was quenched with methanol to trap any ketene intermediates resulting from Wolff rearrangements.<sup>12</sup> One should mention that these substrates gave high conversions of diazo starting materials and the only products formed were either from C-H insertion or Wolff rearrangement.

As mentioned in Section 3.1, the developed model suggests that the carbenes with more electron deficient phenyl rings (i.e. with a smaller PA value) should be more selective for C-H insertion vs. Wolff rearrangement. The provided experimental data is in perfect agreement with the predictions of the model. Indeed, for electron rich 4-MeO-phenyl substituted diazo 1a (PA-value of 237.8 kcal/mol), we find only Wolff product **9a** in 96% yield. Similarly, the tolyl ketone 1b (PA-value of 236.8 kcal/mol) gave only 21% yield of C-H insertion product **8b**, but 71% yield of Wolff rearrangement product **9b**. Further reduction of PA values, i.e. decrease of the electronic property of the phenyl ring, increase selectivity for C-H insertion vs Wolff rearrangement: phenyl ketone 1c (PA-value of 234.9 kcal/mol) provided 34% of 8c; 4-fluorophenyl ketone 1d (PA-value of 234.6 kcal/mol) gave 49% yield of 8d; and 4-chlorophenyl ketone 1e (PA-value of 232.6 kcal/mol) afforded 63% yield

of C-H insertion product **8e**. Through modulation of electronics, the Wolff rearrangement can be suppressed, allowing for more observed C-H insertion.

**Scheme 1**.  $C(sp^3)$ -H Alkylation vs Wolff Rearrangement for 4-Substituted Aryl  $\alpha$ -Diazo- $\beta$ -Ketoesters 1

Next, the other carbonyl classes were evaluated (Scheme 2). In contrast to the clean reactions of the aryl ketones, the reactions with other carbonyl classes did not give appreciable amounts of Wolff rearrangement products and other degradation pathways are evident. In the case of the alkyl ketones, the observed data, again, are consistent with the prediction of the model stating the less steric effects the more C–H insertion product. Indeed, while methyl ketone 1g, with r value of 2.89Å, reacted favorably to form the C-H insertion product was obtained with *t*-butyl ketone 1j, with r value of 3.25 Å. Instead, cyclobutyl ketone 1oj was isolated as the major product resulting from intramolecular C-H insertion into one of the *t*-buyl methyl C-H bonds.<sup>33</sup>

**Scheme 2.** Rh(II)-catalyzed C(sp³)-H Alkylations. **r** values are given in Å.

While the reaction tolerated the ethyl group (as in 1h) to form 8h in  $_{34}\%$  yield, only trace amounts of 8i (from isopropyl ketone 1i) could be detected by NMR analysis of the crude reaction material. These results are fully consistent with our predictive quadrant model. Ketones 1i and 1j are both in Quadrant 2 (Q2) are expected to have poor C-H insertion reactivity due to sterics, whereas ketones 1g and

**1h** are in Quadrant 3 (**Q3**) are expected to have more favorable C-H insertion activity.

Dimethyl diazomalonate  $\mathbf{10}$  is the most commonly studied  $\beta$ -carbonyl ester carbene precursor and its reactivity for intermolecular C-H functionalization has been established in the literature. Consistent with the literature and for our own benchmark data,  $\mathbf{10}$  formed C-H insertion product  $\mathbf{80}$  in 73% yield (Scheme 2).

One tertiary and one secondary amide also were used to validate the model. Unsurprisingly, the sterically-encumbered pyrrolidinyl amide 1s, which is a Q1 substrate, yielded no C-H insertion product. On the other hand, *N*-phenyl amide 1xa (a Q4 substrate) was predicted to have a low barrier to C-H insertion and furnished C-H insertion product in 89% yield.

Intrigued by the favorable secondary amide carbene insertion into the cyclohexane C-H bond, we launched in detail comparable structural and energetic analyses of the tertiary N,N-dimethyl amide 2r and secondary N-methyl amide 2w carbenes (Figure 14). We found that the C-H insertion transition state lies higher in energy for N,N-dimethyl amide carbene ( $\Delta H = 6.5 \text{ kcal/mol}$ ) than secondary amide carbene ( $\Delta H = -2.9 \text{ kcal/mol}$ ). The finding that the secondary amide carbene is more reactive toward C-H bond than tertiary amide carbene is consistent with the reactivity model showing larger r value for N,N-dimethyl amide carbene (3.08 Å) than the secondary amide (2.77 Å). However, close examination of the structures of corresponding C-H insertion transitions state, 3r and 3w, respectively, we also found the 1,6-hydrogen bonding with the 1.99 Å bond distance between the ester oxygen and the amide hydrogen of the secondary amide. Based on these analyses we conclude that 1,6-hydrogen bonding serves as the key factor for decreasing of r value, and, consequently, enables the C-H insertion. Despite convoluting sterics and H-bonding in this instance, **r** succinctly captures reactivity motif by predicting 3w to have smaller relative energy than 3r. A similar change ( $\Delta r = 0.1-0.2$ ) in r is observed when comparing the corresponding esters to the carboxylic acid **3n** ( $\mathbf{r} = 2.67 \text{ Å}$ ), which is also capable of the 1,6-hydrogen bonding.

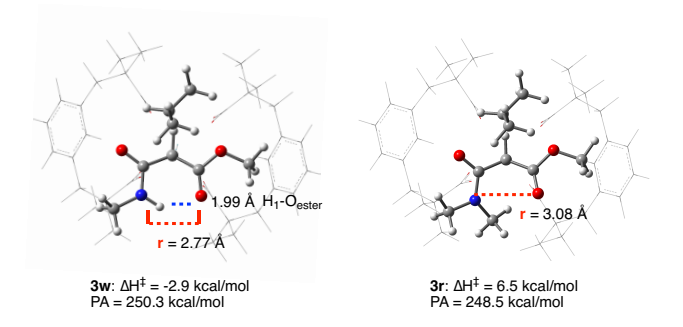


**Figure 14.** Representation of 1,6-Hydrogen bonding interaction in **3w** and comparison with **3r**.

# 6. Reactivity of the Secondary Amides: Scope of Carbenes and Substrates.

In the literature, reactions of carbenes derived from secondary  $\alpha$ -diazo- $\beta$ -amide esters are exceedingly rare. While one report demonstrates that these carbenes can undergo X-H insertions in the presence of a dimeric Rh(II) catalyst,³⁴ to the best of our knowledge, examples of their utility for cyclopropanations (the standard carbene reaction-trapping of C=C double bond) and their capacity to perform C-H insertion reactions (i.e. alkylation) have not been reported.³⁵ Toward this end, we sought to probe the general reactivity potential of secondary  $\alpha$ -diazo- $\beta$ -amide esters.

At first, we explored simple cyclopropanation of styrene with  $\alpha$ -diazo- $\beta$ -amide ester **1xa**. Gratifyingly, we found that the **1xa** reacts with styrene **11** (2 equiv) in the presence of Rh<sub>2</sub>(esp)<sub>2</sub> catalyst to cleanly furnish cyclopropane **12** in 78% yield as a 3:1 mixture of diastereomers (Scheme 3).

**Scheme 3.** Rh(II)-catalyzed cyclopropanation with  $\alpha$ -diazo- $\beta$ -amide ester **1xa** 

To highlight the future potential of the reaction, we employed a chiral dirhodium catalyst complex in hopes of observing enantioselectivity (Scheme 4). When the C-H insertion reaction described above was performed with diazoamide 1xa and cyclohexane in the presence of Rh<sub>2</sub>(*S*-PTAD)<sub>4</sub> (1 mol %), the C-H alkylation product 8xa was obtained in 26% ee (2:1 *er*), albeit with a lower yield (25%). While modest, the enantiomeric excess represents a promising starting point for optimization and catalyst screening.

**Scheme 4**. Asymmetric C-H insertion using a chiral dirhodium catalyst

In an aim to expand scope of the reactive secondary  $\alpha$ -diazo- $\beta$ -amide esters we, again turned to the newly developed reactivity model and calculated PA and  $\bf r$  values for a series of N-aryl-substituted secondary  $\alpha$ -diazo- $\beta$ -amide esters such as  $\bf 1xa$ - $\bf 1xg$  (Figure 15). Across the compounds, PAs varied between 238 and 244 kcal/mol while  $\bf r$  values remained fairly consistent ( $\Delta \bf r$  < 0.03 Å). Therefore, based

the reactivity model, one may expect the secondary amides with lower PA to be more reactive with C–H bond.

Figure 15. Steric (r) and Electronic (PA) Parameters for Various Secondary  $\beta$ -Amide Esters

To validate the predictions of the reactivity model, we synthesized N-aryl-substituted secondary  $\alpha$ -diazo- $\beta$ -amide esters 1xa-1xg and subjected them to the reaction conditions with 5 equiv of cyclohexane (Scheme 4). Once again, general reactivity pattern predicted by the model is fully consistent with experiments. Indeed, the 4-methoxyphenyl substrate 1xb with a larger PA = 244 kcal/mol offered a lower yield (24%). In contrast, the *N*-(4-Cl-phenyl) and N-(4-CF<sub>3</sub>-phenyl) substrates (1xc and 1xd) with PAs of = 240 and 238 kcal/mol, respectively, gave their respective insertion products 8xc and 8xd in 55% and 63% yield. Higher yields (69% and 75%) were observed with the N-(2-Cl-phenyl) and N-(2-CF<sub>3</sub>-phenyl) substrates (**1xe** and **1xf**), respectively. Finally, the N-perfluoro-phenyl amide 1xg with the lowest PA (of 238.0 kcal/mol) afforded the C-H insertion product 8xg in 82% yield. Considering the recent advancements in amide-based directing group C-H functionalization chemistry,36 this series of results are highly auspicious and offer tremendous opportunity for orthogonal and/or tandem reactions.

**Scheme 5**. Rh(II)-catalyzed C-H insertions of diazoamides **1x** 

To expand substrate scope, we also studied the reaction of the reactive N-(2-CF<sub>3</sub>-phenyl) amide  $\mathbf{1xf}$  with pentane (13, instead of cyclohexane) in the presence of  $Rh_2(esp)_2$  catalyst under the similar conditions. Gratifyingly, C(2)-H

and C(3)-H insertion products **14** and **15** were formed in 87% yield with 5.8:1 regioselectivity, respectively. Product **14** was obtained as a 1:1 mixture of diastereomers.

**Scheme 6.** C-H insertion into pentane using 1xf.

## Conclusion

We have introduced accessible parameters such as PA (proton affinity of the carbene carbon),  ${\bf r}$  (the R-O distance in the C-H insertion transition state), and  ${\bf r}'$  (the R-O distance in the anion of the  $\beta$ -carbonyl ester) allowing deconstruction of steric and electronic effects in the  $[Rh_2(esp)_2]$ -catalyzed  $\beta$ -carbonyl ester carbene insertion into the  $C(sp^3)$ -H bond. We used these parameters and developed a chemical-space map and general reactivity model that predicts carbonyl R-substituents which can enhance the C-H insertion.

Following experimental studies have fully validated the predictive power of this model and allowed us to establish: (1) For the **aryl ketones**, selectivity for C-H insertion vs. Wolff rearrangement can be modified by tuning the electronics of the aryl ring; (2) For the alkyl ketones, linear alkyl groups tolerate intermolecular C-H insertion, whereas branched or other sterically-hindered alkyl groups do not; (3) Simple **esters** are both sterically and electronically amenable to intermolecular C-H insertion; (4) The steric bulk of the tertiary amides render them poor performers in intermolecular C-H insertion, and (5) Secondary amides, in contrast, have the highest selectivity for C-H insertion. We showed that the 1.6-hydrogen bonding between the ester oxygen and the amide hydrogen of the secondary amide serves as the key enabling factor for the  $C(sp^3)$ -H alkylation.

Our combined experimental and reactivity predictive model studies led to discovery of the  $[Rh_2(esp)_2]$ -catalyzed both  $C(sp^3)$ -H bond alkylation and C=C double bond cyclopropanation reactions by the secondary N-aryl  $\alpha$ -diazo- $\beta$ -amide esters. We established generality of this new  $C(sp^3)$ -H bond alkylation reaction by expanding it to (a) other secondary N-aryl  $\alpha$ -diazo- $\beta$ -amide esters, and (b) substrates like cyclohexane and pentane. Finally, a promising example of asymmetric induction was also shown using a chiral rhodium catalyst for the cyclopropanation.

# **ASSOCIATED CONTENT**

# **Supporting Information**

Experimental procedures, optimization tables, computational methods used, analytical techniques employed, and copies of NMR spectra (PDF). The Supporting Information is available free of charge on the ACS Publications website.

## **AUTHOR INFORMATION**

# **Corresponding Author**

Email: stefan.france@chemistry.gatech.edu

Email: dmusaev@emory.edu

## **Author Contributions**

The manuscript was written through contributions of all authors. All authors have given approval to the final version of the manuscript.

#### **Notes**

The authors declare no competing financial interests.

## **ACKNOWLEDGMENT**

This work was supported by NSF under the CCI Center for Selective C-H Functionalization (CHE-1700982). B.D.M. thanks NSF for a graduate research fellowship (DGE-1148903). D.G.M. and B.D.M. gratefully acknowledge NSF-MRI-R2 grant (CHE-0958205) and the use of the resources of the Cherry Emerson Center for Scientific Computation.

## **REFERENCES**

- (1) Davies, H. M. L. and B. T. Parr in *Contemporary Carbene Chemistry*, John Wiley & Sons, Inc., 2013, pp. 363-403.
- (2) Guy Bertrand. Carbene Chemistry: From Fleeting Intermediates to Powerful Reagents. CRC Press. 2002.
- (3) Brookhart, M.; Studabaker, W. B. Cyclopropanes from Reactions of Transition Metal Carbene Complexes with Olefins. *Chem. Rev.* 1987, 87, 411.
- (4) Doyle, M. P.; Forbes, D. C. Recent Advances in Asymmetric Catalytic Metal Carbene Transformations. *Chem. Rev.* **1998**, *98*, 911.
- (5) Doyle, M. P.; Duffy, R.; Ratnikov, M.; Zhou, L. Catalytic Carbene Insertion into C-H Bonds. *Chem. Rev.* **2010**, *110*, 704.
- (6) Audia, J. E.; Droste J. J.; Gevorgyan, V.; Rubin, M.; Chan, W.; Yu, W.; McLarney, B.; France, S. (2016) "Dimethyl Diazomalonate." *Encyclopedia of Reagents for Organic Synthesis*. John Wiley & Sons. Ltd.
- (7) Lindsay, V. N. G.; Nicolas, C.; Charette, A. B. Asymmetric Rh(II)-Catalyzed Cyclopropanation of Alkenes with Diacceptor Diazo Compounds: *p*-Methoxyphenyl Ketone as a General Stereoselectivity Controlling Group. *J. Am. Chem. Soc.* **2011**, *133*, 8972.
- (8) McLarney, B. D.; Cavitt, M. A.; Donnell, T. M.; Musaev, D. G.; France, S. Rh(II)-Catalyzed  $\beta$ -C(sp²)-H Alkylation of Enol Ethers, Enamides and Enecarbamates with  $\alpha$ -Diazo Dicarbonyl Compounds. *Chem. Eur. J.* **2017**, 23, 1129.
- (9) England, D. B.; Eagan, J. M.; Merey, G.; Anac, O.; Padwa, A. The Rhodium(II) Carbenoid Cyclization-Cycloaddition Cascade of Alpha-Diazo Dihydroindolinones for the Synthesis of Novel Azapolycyclic Ring Systems. *Tetrahedron* **2008**, *64*, 988.
- (10) Davies, H. M. L.; Morton, D. Guiding Principles for Site Selective and Stereoselective Intermolecular C-H Functionalization by Donor/acceptor Rhodium Carbenes. *Chem. Soc. Rev.* **2011**, *40*, 1857.
- (11) Davies, H. M. L.; Beckwith, R. E. J. Catalytic Enantioselective C-H Activation by Means of Metal-Carbenoid-Induced C-H Insertion. *Chem. Rev.* **2003**, 103, 2861.
- (12) Kirmse, W. 100 Years of the Wolff Rearrangement. Eur. J. Org. Chem. 2002, 2002, 2193.
- (13) Scott, A. P.; Platz, M. S.; Radom, L. Singlet–Triplet Splittings and Barriers to Wolff Rearrangement for Carbonyl Carbenes. *J. Am. Chem. Soc.* **2001**, *123*, 6069.

- (14) Gronert, S.; Keeffe, J. R.; More O'Ferrall, R. A. Stabilities of Carbenes: Independent Measures for Singlets and Triplets. *J. Am. Chem. Soc.* **2011**, *1*33, 3381.
- (15) Padwa, A.; Hornbuckle, S. F. Ylide Formation from the Reaction of Carbenes and Carbenoids with Heteroatom Lone Pairs. *Chem. Rev.* **1991**, *91*, 263.
- (16) (a) Watanabe, N.; Masashio, A.; Hashimoto, S.-I.; Ikegami, S. Enantioselective Intramolecular C-H Insertion Reactions of N-Alkyl-N-tert-butyl-α-methoxycarbonyl-α-diazoacetamides Catalyzed by Dirhodium(II) Carboxylates: Catalytic, Asymmetric Construction of 2-Azetidinones. Synlett 1994, 12, 1031; (b) Anada, M.; Hashimoto, S.-I. Enantioselective Synthesis of 4-Substituted 2-Pyrrolidinones by Site-selective C-H Insertion of α-Methoxycarbonyl-α-diazoacetanilides Catalyzed by Dirhodium(II) Tetrakis[N-phthaloyl-(S)-tert-leucinate]. Tetrahedron Lett. 1998, 39, 79; (c) Anada, M.; Hashimoto, S.-I. Enantioselective Intramolecular C-H Insertion Route to a Key Intermediate for the Synthesis of Trinem Antibiotics. Tetrahedron Lett. 1998, 39, 9063; (d) Anada, M.; Watanabe, N. Highly Enantioselective Construction of the Key Azetidin-2-ones for the Synthesis of Carbapenem Antibiotics via Intramolecular C-H Insertion Reactions of  $\alpha$ -Methoxycarbonyl-α-diazoacetamides Catalyzed by Chiral Dirhodium(II) Carboxylates. Chem. Commun. 1998, 1517.
- (17) Cui, X.; Xu, X.; Jin, L.-M.; Wojtas, L.; Zhang, X. P. Stereoselective Radical C-H Alkylation with Acceptor/Acceptor-Substituted Diazo Reagents via Co(II)-Based Metalloradical Catalysis. *Chem. Sci.* **2015**, *6*, 1219.
- (18) H. M. L. Davies and A. M. Walji, in *Modern rhodium-catalyzed organic reactions*, ed. P. A. Evans, Wiley-VCH, Weinheim, 2005, pp. 301-337.
- (19) Nani, R. R.; Reisman, S. E. α-Diazo-β-ketonitriles: Uniquely Reactive Substrates for Arene and Alkene Cyclopropanation. *J. Am. Chem. Soc.* **2013**, *13*5, 7304.
- (20) Doyle, M. P.; Hu, W.; Wee, A. G. H.; Wang, Z.; Duncan, S. C. Influences of Catalyst Configuration and Catalyst Loading on Selectivities in Reactions of Diazoacetamides. Barrier to Equilibrium Between Diastereomeric Conformations. *Org. Lett.* **2003**, *5*, 407.
- (21) Zhang, B.; Wee, A. G. H. Conformational, Steric and Electronic Effects on the Site- and Chemoselectivity of the Metal-catalyzed Reaction of N-Bis(trimethylsilyl)methyl, N-(2-Indolyl)methyl α-Diazoamides. *Org. Biomol. Chem.* **2012**, *10*, 4597.
- (22) Muller, P.; Tohill, S. Intermolecular Cyclopropanation Versus CH Insertion in RhII-catalyzed Carbenoid Reactions. *Tetrahedron* 2000, 56, 1725.
- (23) Davies, H. M. L.; Hansen, T. Asymmetric Intermolecular Carbenoid C-H Insertions Catalyzed by Rhodium(II) (S)-N-(p-Dodecylphenyl)sulfonylprolinate. *J. Am. Chem. Soc.* **1997**, *119*, 19075.
- (24) Nakamura, E.; Yoshikai, N.; Yamanaka, M. Mechanism of C-H Bond Activation/C-C Bond Formation Reaction between Diazo Compound and Alkane Catalyzed by Dirhodium Tetracarboxylate. J. Am. Chem. Soc. 2002, 124, 7181
- (25) (a) Taber, D. F.; Ruckle, R. E., Jr. Cyclopentane Construction by Dirhodium Tetraacetate-mediated Intramolecular C-H Insertion: Steric and Electronic Effects. *J. Am. Chem. Soc.* **1986**, *108*, 7686; (b) Doyle, M. P.; Westrum, L. J.; Wolthuis, W. N. E.; See, M. M.; Boone, W. P.; Bagheri, V.; Pearson, M. M. Electronic and Steric Control in Carbon-hydrogen Insertion Reactions of Diazoaceto-acetates Catalyzed by Dirhodium(II) Carboxylates and Carbox-amides. *J. Am. Chem. Soc.* **1993**, *115*, 958; (c) Davies, H. M. L.; Ren, P.; Jin, Q. Catalytic Asymmetric Allylic C-H Activation as a Surrogate of the Asymmetric Claisen Rearrangement. *Org. Lett.* **2001**, *3*, 3587.
- (26) For relevant literature on predictive reactivity modeling studies, see: (a) Zhao, S.; Gensch, T.; Murray, B.; Niemeyer, Z. L.; Sigman, M. S.; Biscoe, M. R. Enantiodivergent Pd-catalyzed C-C

Bond Formation Enabled Through Ligand Parameterization. Science 2018, 362, 670-674; (b) Metsänen, T. T.; Lexa, K. W.; Santiago, C. B.; Chung, C. K.; Xu, Y.; Liu, Z.; Humphrey, G. R.; Ruck, R. T.; Sherer, E. C.; Sigman, M. S. Combining Traditional 2D and Modern Physical Organic-derived Descriptors to Predict Enhanced Enantioselectivity for the Key Aza-Michael Conjugate Addition in the Synthesis of Prevymis<sup>™</sup> (Letermovir). *Chem. Sci.* **2018**, *9*, 6922-6928; (c) Santiago, C. B.; Guo, J.-Y.; Sigman, M. S. Predictive and Mechanistic Multivariate Linear Regression Models for Reaction Development. Chem. Sci. 2018, 35, 2398-2412; (d) Gormisky, P. E.; White, M. C. Catalyst-Controlled Aliphatic C–H Oxidations with a Predictive Model for Site-Selectivity. J. Am. Chem. Soc. 2013, 135, 14052-14055; (e) Goetz, A. E.; Sarah M. Bronner, S. M.; Cisneros, J. D.; Joshua M. Melamed, J. M.; Paton, R. S.; Houk, K. N.; Garg, N. K. An Efficient Computational Model to Predict the Synthetic Utility of Heterocyclic Arynes. Angew. Chem. Int. Ed. 2012, 51, 2758-2762; (f) Maldonado, A. G.; Rothenberg, G. Predictive Modeling in Homogeneous Catalysis: A Tutorial. Chem. Soc. Rev. 2010, 39, 1891-1902.

(27) (a) Gaussian 09, Revision D.01, M. J. Frisch, G. W. Trucks, H. B. Schlegel, G. E. Scuseria, M. A. Robb, J. R. Cheeseman, G. Scalmani, V. Barone, B. Mennucci, G. A. Petersson, H. Nakatsuji, M. Caricato, X. Li, H. P. Hratchian, A. F. Izmaylov, J. Bloino, G. Zheng, J. L. Sonnenberg, M. Hada, M. Ehara, K. Toyota, R. Fukuda, J. Hasegawa, M. Ishida, T. Nakajima, Y. Honda, O. Kitao, H. Nakai, T. Vreven, J. A. Montgomery, Jr., J. E. Peralta, F. Ogliaro, M. Bearpark, J. J. Heyd, E. Brothers, K. N. Kudin, V. N. Staroverov, R. Kobayashi, J. Normand, K. Raghavachari, A. Rendell, J.C. Burant, S.S. Iyengar, J. Tomasi, M. Cossi, N. Rega, J. M. Millam, M. Klene, J. E. Knox, J. B. Cross, V. Bakken, C. Adamo, J. Jaramillo, R. Gomperts, R. E. Stratmann, O. Yazyev, A. J. Austin, R. Cammi, C. Pomelli, J. W. Ochterski, R. L. Martin, K. Morokuma, V. G. Zakrzewski, G. A. Voth, P. Salvador, J. J. Dannenberg, S. Dapprich, A. D. Daniels, Ö. Farkas, J. B. Foresman, J. V. Ortiz, J. Cioslowski, and D. J. Fox, Gaussian, Inc., Wallingford CT, 2013; (b) Chai, J.-D.; Head-Gordon, M. Long-range Corrected Hybrid Density Functionals with Damped Atom-Atom Dispersion Corrections. Phys. Chem. Chem. Phys. 2008, 10, 6615; (c) Wadt, W. R.; Hay, P. J. Ab Initio Effective Core Potentials for Molecular Calculations. Potentials for Main Group Elements Sodium to Bismuth. J. Chem. Phys. 1985, 82, 284; (d) Hay, P. J.; Wadt, W. R. Ab Initio Effective Core Potentials for Molecular Calculations. Potentials for the Transition Metal Atoms Scandium to Mercury. J. Chem. Phys. 1985, 82,

(28) (a) Tomasi, J.; Mennucci, B.; Cammi, R. Quantum Mechanical Continuum Solvation Models. *Chem. Rev.* **2005**, *105*, 2999 and references cited therein; (b) Tomasi, J.; Mennucci, B. Cances, E. The IEF Version of the PCM Solvation Method: An Overview of a

New Method Addressed to Study Molecular Solutes at the QM Ab Initio Level. *THEOCHEM* **1999**, *464*, 211; (c) Pascal-Ahuir, J.L.; Silla, E.; Tuñoń, I. GEPOL: An Improved Description of Molecular Surfaces. III. A New Algorithm for the Computation of a Solvent-excluding Surface. *J. Comput. Chem.* **1994**, *15*, 1127.

- (29) Hammett, L. P. Effect of Structure upon the Reactions of Organic Compounds. Benzene Derivatives. *J. Am. Chem. Soc.* **1937**, 59, 96.
- (30) PA represents the enthalpy change in the reaction between an anion or neutral species and a proton. For a detailed review, see: Maksic, Z. B.; Kovacevic, B.; Vianello, R. Advances in Determining the Absolute Proton Affinities of Neutral Organic Molecules in the Gas Phase and Their Interpretation: A Theoretical Account. *Chem. Rev.* 2012, 112, 5240-5270.
- (31) Anslyn, E. V. and Dougherty, D. A. in *Modern Physical Organic Chemistry*. Sausalito, CA: University Science Books, 2006, pp. 104-105.
- (32) MATLAB and Statistics Toolbox Release 2017b, The Math-Works, Inc., Natick, Massachusetts, United States.
- (33) (a) Cheng, Q.-Q.; Deng, Y.; Lankelma, M.; Doyle, M. P. Cycloaddition Reactions of Enoldiazo Compounds. *Chem. Soc. Rev.* **2017**, *46*, 5425; (b) Pitts, C. R.; Lectka, T. Chemical Synthesis of  $\beta$ -Lactams: Asymmetric Catalysis and Other Recent Advances. *Chem. Rev.* **2014**, *114*, 7930.
- (34) Trstenjak, U.; Ilas, J.; Kikelj, D. Studies Towards the Synthesis of Alkyl N-(4-Nitrophenyl)-3/2-oxomorpholine-2/3-carboxylates. *Helv. Chim. Acta* **2013**, *96*, 2160.
- (35) While Zhang reported the Co-catalyzed metalloradical cyclopropenation of alkynes using α-cyanodiazoacetamides, the method involves a radical mechanism and doesn't involve carbenes. For more detail, see: Cui, X.; Xu, X.; Lu, H.; Zhu, S.; Wojtas, L.; Zhang, X. P. Enantioselective Cyclopropenation of Alkynes with Acceptor/Acceptor-Substituted Diazo Reagents via Co(II)-Based Metalloradical Catalysis. *J. Am. Chem. Soc.* **2011**, *1*33, 3304.
- (36) (a) Wu, Q.-F.; Wang, X.-B.; Shen, P.-X.; Yu, J.-Q. Enantioselective C-H Arylation and Vinylation of Cyclobutyl Carboxylic Amides. *ACS Catal.* **2018**, *8*, 2577; (b) Zhu, R.-Y.; Saint-Denis, T. G.; Shao, Y.; He, J.; Sieber, J. D.; Senanayake, C. H.; Yu, J.- Q. Ligand-Enabled Pd(II)-Catalyzed Bromination and Iodination of C(sp3)-H Bonds. *J. Am. Chem. Soc.* **2017**, *139*, 5724; (c) Daugulis, O.; Roane, J.; Tran, L. D. Bidentate, Monoanionic Auxiliary-Directed Functionalization of Carbon-Hydrogen Bonds. *Acc. Chem. Res.* **2015**, 48, 1053; (d) Rouquet, G.; Chatani, N. Catalytic Functionalization of C(sp2)-H and C(sp3)-H Bonds by Using Bidentate Directing Groups. *Angew. Chem. Int. Ed.* **2013**, 52, 11726.